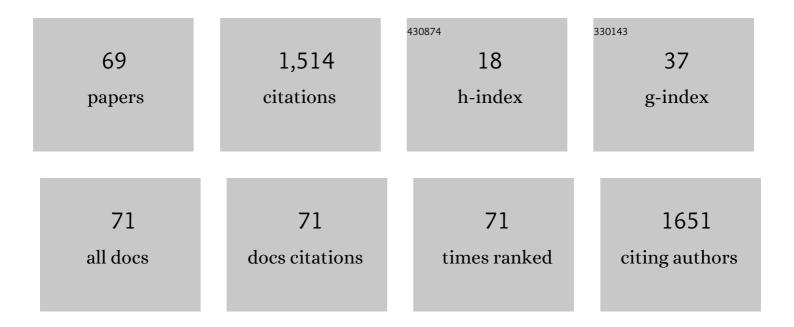
List of Publications by Year in descending order

Source: https://exaly.com/author-pdf/6501598/publications.pdf Version: 2024-02-01



HENDRIK I VOS

#	Article	IF	CITATIONS
1	Acoustic behavior of microbubbles and implications for drug delivery. Advanced Drug Delivery Reviews, 2014, 72, 28-48.	13.7	295
2	Acoustic droplet vaporization is initiated by superharmonic focusing. Proceedings of the National Academy of Sciences of the United States of America, 2014, 111, 1697-1702.	7.1	159
3	Lipid Shedding from Single Oscillating Microbubbles. Ultrasound in Medicine and Biology, 2014, 40, 1834-1846.	1.5	71
4	A Front-End ASIC With Receive Sub-array Beamforming Integrated With a \$32 imes 32\$ PZT Matrix Transducer for 3-D Transesophageal Echocardiography. IEEE Journal of Solid-State Circuits, 2017, 52, 994-1006.	5.4	70
5	Nonspherical Shape Oscillations of Coated Microbubbles inÂContact With a Wall. Ultrasound in Medicine and Biology, 2011, 37, 935-948.	1.5	65
6	A Prototype PZT Matrix Transducer With Low-Power Integrated Receive ASIC for 3-D Transesophageal Echocardiography. IEEE Transactions on Ultrasonics, Ferroelectrics, and Frequency Control, 2016, 63, 47-59.	3.0	60
7	Cardiac Shear Wave Velocity Detection in the Porcine Heart. Ultrasound in Medicine and Biology, 2017, 43, 753-764.	1.5	50
8	Method for Microbubble Characterization Using Primary Radiation Force. IEEE Transactions on Ultrasonics, Ferroelectrics, and Frequency Control, 2007, 54, 1333-1345.	3.0	48
9	A Pitch-Matched Front-End ASIC With Integrated Subarray Beamforming ADC for Miniature 3-D Ultrasound Probes. IEEE Journal of Solid-State Circuits, 2018, 53, 3050-3064.	5.4	43
10	4-D Echo-Particle Image Velocimetry in a Left Ventricular Phantom. Ultrasound in Medicine and Biology, 2020, 46, 805-817.	1.5	38
11	Detection of Contrast Agents: Plane Wave Versus Focused Transmission. IEEE Transactions on Ultrasonics, Ferroelectrics, and Frequency Control, 2016, 63, 203-211.	3.0	37
12	Cardiac Shear Wave Elastography Using a Clinical Ultrasound System. Ultrasound in Medicine and Biology, 2017, 43, 1596-1606.	1.5	37
13	Effect of Clot Stiffness on Recombinant Tissue Plasminogen Activator Lytic Susceptibility in Vitro. Ultrasound in Medicine and Biology, 2018, 44, 2710-2727.	1.5	35
14	A Reconfigurable Ultrasound Transceiver ASIC With <inline-formula> <tex-math notation="LaTeX">\$24imes40\$ </tex-math </inline-formula> Elements for 3-D Carotid Artery Imaging. IEEE Journal of Solid-State Circuits, 2018, 53, 2065-2075.	5.4	30
15	Naturally Occurring Shear Waves in Healthy Volunteers and Hypertrophic Cardiomyopathy Patients. Ultrasound in Medicine and Biology, 2019, 45, 1977-1986.	1.5	23
16	Combining Ultrafast Ultrasound and High-Density EMG to Assess Local Electromechanical Muscle Dynamics: A Feasibility Study. IEEE Access, 2021, 9, 45277-45288.	4.2	23
17	Assessing cardiac stiffness using ultrasound shear wave elastography. Physics in Medicine and Biology, 2022, 67, 02TR01.	3.0	22
18	High Frame Rate Ultrasound Particle Image Velocimetry for Estimating High Velocity Flow Patterns in the Left Ventricle. IEEE Transactions on Ultrasonics, Ferroelectrics, and Frequency Control, 2018, 65, 2222-2232.	3.0	21

#	Article	IF	CITATIONS
19	High-Frame-Rate Echo-Particle Image Velocimetry Can Measure the High-Velocity Diastolic Flow Patterns. Circulation: Cardiovascular Imaging, 2019, 12, e008856.	2.6	20
20	<i>F</i> – <i>k</i> Domain Imaging for Synthetic Aperture Sequential Beamforming. IEEE Transactions on Ultrasonics, Ferroelectrics, and Frequency Control, 2016, 63, 60-71.	3.0	19
21	Self-demodulation of high-frequency ultrasound. Journal of the Acoustical Society of America, 2010, 127, 1208-1217.	1.1	18
22	High-Frame-Rate Contrast-enhanced US Particle Image Velocimetry in the Abdominal Aorta: First Human Results. Radiology, 2018, 289, 119-125.	7.3	18
23	High-Frame-Rate Contrast-Enhanced Ultrasound for Velocimetry in the Human Abdominal Aorta. IEEE Transactions on Ultrasonics, Ferroelectrics, and Frequency Control, 2018, 65, 2245-2254.	3.0	18
24	High Frame Rate Volumetric Imaging of Microbubbles Using a Sparse Array and Spatial Coherence Beamforming. IEEE Transactions on Ultrasonics, Ferroelectrics, and Frequency Control, 2021, 68, 3069-3081.	3.0	17
25	Focal areas of increased lipid concentration on the coating of microbubbles during short tone-burst ultrasound insonification. PLoS ONE, 2017, 12, e0180747.	2.5	17
26	Contrast-Enhanced High-Frame-Rate Ultrasound Imaging of Flow Patterns in Cardiac Chambers and Deep Vessels. Ultrasound in Medicine and Biology, 2020, 46, 2875-2890.	1.5	15
27	Early detection of left ventricular diastolic dysfunction using conventional and speckle tracking echocardiography in a large animal model of metabolic dysfunction. International Journal of Cardiovascular Imaging, 2017, 34, 743-749.	1.5	13
28	Myocardial Stretch Post-atrial Contraction in Healthy Volunteers and Hypertrophic Cardiomyopathy Patients. Ultrasound in Medicine and Biology, 2019, 45, 1987-1998.	1.5	13
29	The effect of size range on ultrasound-induced translations in microbubble populations. Journal of the Acoustical Society of America, 2020, 147, 3236-3247.	1.1	12
30	Ultrasound-Mediated Drug Delivery With a Clinical Ultrasound System: In Vitro Evaluation. Frontiers in Pharmacology, 2021, 12, 768436.	3.5	12
31	Preclinical Testing of Frequency-Tunable Capacitive Micromachined Ultrasonic Transducer Probe Prototypes. Ultrasound in Medicine and Biology, 2017, 43, 2079-2085.	1.5	11
32	A direct comparison of natural and acoustic-radiation-force-induced cardiac mechanicalÂwaves. Scientific Reports, 2020, 10, 18431.	3.3	11
33	Parasternal Versus Apical View in Cardiac Natural Mechanical Wave Speed Measurements. IEEE Transactions on Ultrasonics, Ferroelectrics, and Frequency Control, 2020, 67, 1590-1602.	3.0	11
34	Calibrating Doppler Imaging of Preterm Intracerebral Circulation Using a Microvessel Flow Phantom. Frontiers in Human Neuroscience, 2015, 8, 1068.	2.0	10
35	High-Frame-Rate Power Doppler Ultrasound Is More Sensitive than Conventional Power Doppler in Detecting Rheumatic Vascularisation. Ultrasound in Medicine and Biology, 2017, 43, 1868-1879.	1.5	9
36	Quantitative imaging performance of frequency-tunable capacitive micromachined ultrasonic transducer array designed for intracardiac application: Phantom study. Ultrasonics, 2018, 84, 421-429.	3.9	9

#	Article	IF	CITATIONS
37	Plane-Wave Contrast Imaging: A Radiation Force Point of View. IEEE Transactions on Ultrasonics, Ferroelectrics, and Frequency Control, 2018, 65, 2296-2300.	3.0	9
38	Microbubble Radiation Force-Induced Translation in Plane-Wave Versus Focused Transmission Modes. IEEE Transactions on Ultrasonics, Ferroelectrics, and Frequency Control, 2019, 66, 1856-1865.	3.0	9
39	Receive/Transmit Aperture Selection for 3D Ultrasound Imaging with a 2D Matrix Transducer. Applied Sciences (Switzerland), 2020, 10, 5300.	2.5	9
40	Revealing Intraosseous Blood Flow in the Human Tibia With Ultrasound. JBMR Plus, 2021, 5, e10543.	2.7	9
41	Spatiotemporal Distribution of Nanodroplet Vaporization in a Proton Beam Using Real-Time Ultrasound Imaging for Range Verification. Ultrasound in Medicine and Biology, 2022, 48, 149-156.	1.5	9
42	Native blood speckle vs ultrasound contrast agent for particle image velocimetry with ultrafast ultrasound - in vitro experiments. , 2016, , .		8
43	Parametric array technique for microbubble excitation. IEEE Transactions on Ultrasonics, Ferroelectrics, and Frequency Control, 2011, 58, 924-934.	3.0	7
44	Synthetic Aperture Sequential Beamforming for phased array imaging. , 2015, , .		7
45	Sparse Volumetric PZT Array with Density Tapering. , 2018, , .		7
46	Acoustic characterization of a miniature matrix transducer for pediatric 3D transesophageal echocardiography. Ultrasound in Medicine and Biology, 2018, 44, 2143-2154.	1.5	7
47	Design of an Ultrasound Transceiver ASIC with a Switching-Artifact Reduction Technique for 3D Carotid Artery Imaging. Sensors, 2021, 21, 150.	3.8	7
48	A Compact Integrated High-Voltage Pulser Insensitive to Supply Transients for 3-D Miniature Ultrasound Probes. IEEE Solid-State Circuits Letters, 2022, 5, 166-169.	2.0	7
49	Fast Volumetric Imaging Using a Matrix Transesophageal Echocardiography Probe with Partitioned Transmit–Receive Array. Ultrasound in Medicine and Biology, 2018, 44, 2025-2042.	1.5	5
50	Local myocardial stiffness variations identified by high frame rate shear wave echocardiography. Cardiovascular Ultrasound, 2020, 18, 40.	1.6	5
51	Optimization of Microbubble Concentration and Acoustic Pressure for Left Ventricular High-Frame-Rate EchoPIV in Patients. IEEE Transactions on Ultrasonics, Ferroelectrics, and Frequency Control, 2021, 68, 2432-2443.	3.0	4
52	Experimental Investigation of the Effect of Subdicing on an Ultrasound Matrix Transducer. , 2021, , .		3
53	Acoustic Modulation Enables Proton Detection With Nanodroplets at Body Temperature. IEEE Transactions on Ultrasonics, Ferroelectrics, and Frequency Control, 2022, 69, 2028-2038.	3.0	3
54	Left ventricular high frame rate echo-particle image velocimetry: clinical application and comparison with conventional imaging. Cardiovascular Ultrasound, 2022, 20, 11.	1.6	3

#	Article	IF	CITATIONS
55	Imaging Scheme for 3-D High-Frame-Rate Intracardiac Echography: A Simulation Study. IEEE Transactions on Ultrasonics, Ferroelectrics, and Frequency Control, 2022, 69, 2862-2874.	3.0	3
56	Dual stage beamforming in the absence of front-end receive focusing. Physics in Medicine and Biology, 2017, 62, 6631-6648.	3.0	2
57	3D high frame rate flow measurement using a prototype matrix transducer for carotid imaging. , 2019, , .		2
58	Two-Stage Beamforming for Phased Array Imaging Using the Fast Hankel Transform. IEEE Transactions on Ultrasonics, Ferroelectrics, and Frequency Control, 2019, 66, 297-308.	3.0	2
59	Impact of Bit Errors in Digitized RF Data on Ultrasound Image Quality. IEEE Transactions on Ultrasonics, Ferroelectrics, and Frequency Control, 2020, 67, 13-24.	3.0	2
60	A 1.2mW/channel 100µm-Pitch-Matched Transceiver ASIC with Boxcar-Integration-Based RX Micro-Beamformer for High-Resolution 3D Ultrasound Imaging. , 2022, , .		2
61	A Study of Radiation Force Effects in Plane-Wave Transmission Mode. , 2018, , .		1
62	A comparison of natural and acoustic radiation force induced shear wave propagation speed measurements in open-chest pigs. , 2019, , .		1
63	Independent Component Analysis Filter for Small Vessel Contrast Imaging During Fast Tissue Motion. IEEE Transactions on Ultrasonics, Ferroelectrics, and Frequency Control, 2022, 69, 2282-2292.	3.0	1
64	Towards 3D ultrasound imaging of the carotid artery using a programmable and tileable matrix array. , 2017, , .		0
65	Virtually Extended Array Imaging Improves Lateral Resolution in High Frame Rate Volumetric Imaging. , 2018, , .		0
66	Frequency Domain Two-Stage Beamforming for Phased Array Imaging Using the Fast Hankel Transform. , 2018, , .		0
67	Numerical model of Lamb wave propagation in the tapered septal wall of the heart. Proceedings of Meetings on Acoustics, 2019, , .	0.3	0
68	Direction-independent bulk shear wave speed in 3D. , 2019, , .		0
69	Design of a Dual Frequency Probe for Photoacoustic Imaging of the Carotid Artery. , 2020, , .		0